Theoretical study on the reaction path and rate constants of the hydrogen atom abstraction reaction of CH 2O with CH 3/OH

ARTICLE *in* CHEMICAL PHYSICS · DECEMBER 2004

Impact Factor: 1.65 · DOI: 10.1016/j.chemphys.2004.07.014

5 AUTHORS, INCLUDING:

Min pu
Beijing University of Chemical Technology
52 PUBLICATIONS **561** CITATIONS

SEE PROFILE

Available online at www.sciencedirect.com
SCIENCE DIRECT®
Chemical Physics 307 (2004) 35–43
Chemical Physics
www.elsevier.com/locate/chemphys

Theoretical study on the reaction path and rate constants of the hydrogen atom abstraction reaction of CH_2O with CH_3/OH

Hui-Ying Li [a], Min Pu [a,*], Yong-Qiang Ji [b], Zhen-Feng Xu [a], Wen-Lin Feng [a]

[a] *Key Laboratory of Science and Technology of Controllable Chemical Reactions, Ministry of Education, Beijing University of Chemical Technology, Beijing 100029, China*
[b] *College of Chemistry and Chemical Engineering, Ningxia University, YinChuan 750021, China*

Received 1 June 2004; accepted 15 July 2004
Available online 11 September 2004

Abstract

The direct dynamics of the hydrogen abstraction reactions of CH_2O with CH_3/OH are studied using ab initio molecular orbital theory. Both the geometry optimizations of all the stationary points and the vibrational frequency calculations are carried out at the UQCISD/6-311G(d,p) level. The single-point energy is obtained by the multicoefficient Gaussian 3-version 3s (MCG3/3) method. The analysis to the changes of the interatomic distances on the minimum energy paths show that, the breaking of C–H bonds of CH_2O and (i) the forming of C–H bond of CH_4 in the reaction of CH_2O with CH_3, (ii) the forming of O–H bond of H_2O in the reaction of CH_2O with OH, are both concerted. For each reaction, there exists a reactive vibrational normal-mode, and its frequencies change is relevant to the forming and breaking of the above covalent bond. Furthermore, the theoretical forward reaction rate constants in the temperature range 300–3000 K are computed by canonical variational transition state theory with small-curvature tunneling correction (CVT/SCT) method. The computed values of the rate constants are in good agreement with the available experimental data in the measured temperature range. Moreover, the tunneling effects are found to contribute significantly to the rate constants at low temperatures.

1. Introduction

Formaldehyde (CH_2O) is an important intermediate in the oxidation of aldehydes, alcohols, ethers and hydrocarbons in general [1,2], and it is particularly a significant pro-knock additive of the methane-base fuel [3,4]. Moreover, the thermodynamic stability of formaldehyde leads to large accumulation in air and finally pollution, and it causes a concern environmentally [5]. In combustion, CH_2O is either formed readily by the oxidation of hydrocarbons or removed rapidly by various radicals, such as H, O, OH, CH_3. Therefore, the hydrogen abstraction reactions of formaldehyde with methyl and hydroxyl,

$$CH_2O + CH_3 \rightarrow CHO + CH_4 \quad (1)$$

$$CH_2O + OH \rightarrow CHO + H_2O \quad (2)$$

have attracted much interest of both atmospheric and combustion chemists [6,7].

Reactions (1) and (2) have been widely investigated experimentally in the past decades. Reaction (1) has been studied by several experimental methods [7–10] over a wide temperature range of 300–2000 K. The Arrhenius plot of reaction (1) shows nonlinear behavior [8]. The kinetics of reaction (2) has been studied either directly at low temperatures [5,6,11–14] or indirectly at high temperatures [15,16]. Lin [5] reported direct measurements of reaction (2) over the temperature 296–576

* Corresponding author. Tel.: +86 10 6444 5393; fax: +86 10 6442 5385.
E-mail address: pumin@mail.buct.edu.cn (M. Pu).

0301-0104/$ - see front matter © 2004 Elsevier B.V. All rights reserved.
doi:10.1016/j.chemphys.2004.07.014

K and extrapolated a nonlinear Arrhenius plot into the combustion range 300–2500 K.

On the theoretically approaches, Franciso et al. [17,18] gave the activation energy for reactions (1) and (2) at UMP2/6-311G(d,p) level (10.60 and 1.20 kcal/mol, respectively). Page et al. [19] used ab initio multi-configuration self-consistent-field (MCSCF) and multi-reference configuration interaction (MRCI) method to investigate the potential energy surface for reaction (2), and gave a activation energy of 3.60 kcal/mol and a reaction exothermicity of 21.70 kcal/mol. However, little information has been given on the reaction paths and rate constants that could describe the detailed reaction mechanism.

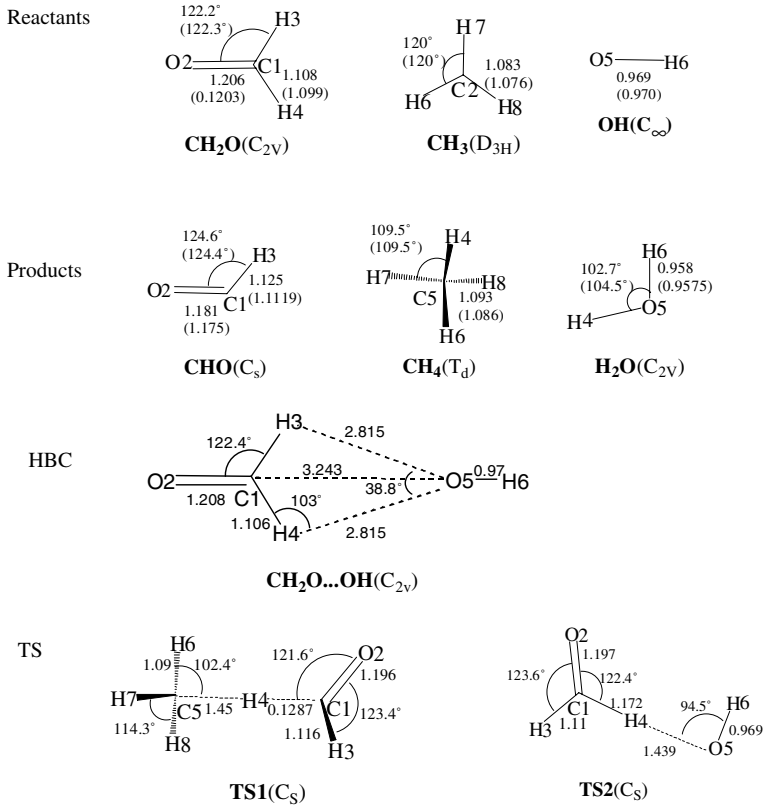

Fig. 1. Optimized geometric parameters (bond lengths in (Å) and angles in (°)) of the reactants, products, hydrogen-bonded complex (HBC) and transition states at the UQCISD/6-311G(d,p) level. The values in the parentheses are the experimental values.

Table 1
Calculated harmonic frequencies (in cm^{-1}) of the reactants, product, and transition state of the two reactions at the QCISD/6-311G(d,p) level

Species	QCISD/6-311G(d,p)	Expt. [35,36]
CH_2O	2862.6, 2807.9, 1729.9, 1493.7, 1230.5, 1151.1	2997, 2978, 1778, 1529, 1299, 1191
CH_3	3154.8, 3154.8, 2981.5, 1369.9, 1369.9, 414.1	3002, 3002, 3184, 1383, 1383, 580
OH	3615.5	3735
CHO	2572.0, 1817.0, 1095.1	2790, 1920, 1126
CH_4	3019.7, 3019.7, 3019.7, 2905.2, 1500.4, 1500.4, 1303.7, 1303.7, 1303.7	3019, 3019, 3019, 2917, 1534, 1534, 1306, 1306, 1306
H_2O	3808.7, 3719.0, 1610.0	3756, 3657, 1596
$CH_2O\cdots OH$(HBC)	3625.9, 2895.5, 2825.6, 1726.5, 1481.2, 1232.2 1157.0, 193.98, 129.51, 111.77, 80.683, 105.2*i*	
TS1	3075.6, 3071.7, 2937.8, 2725.3, 1750.6, 1430.4, 1389.3, 1380.5, 1231.8, 1214, 1080.7, 592.34, 557.34, 457.01, 256.35, 126.13, 32.044, 1828.9*i*	
TS2	3615.7, 2816.3, 1771.2, 1482.6, 1346.0, 1225.5, 1037.1, 713.18, 160.79, 130.18, 61.418, 678.1*i*	

Scale factor, 0.9537 [34].

In present work, the ab intio molecular orbital theory with configuration interaction at higher level QCISD/6-311(d,p) are used to investigate the above hydrogen abstraction reactions (1) and (2) for the reaction paths. The variational transition state theory (VTST) [20–22] is applied to calculate the reaction rate constants over a wide temperature range. The canonical variational transition state theory (CVT) and the small-curvature tunneling (SCT) method [23] have been taken into account at the VTST. The comparisons between the theoretical rate constants and the experimental values will be discussed. A detailed dynamics study on the title reactions is expected not only to accumulate the rate constant data of the formaldehyde reactions, but also to gain deeper insight into the reactivity of the hydrogen abstraction about formaldehyde. Adopting the above QCISD/6-311(d,p) and CVT/SCT methods, we recently have obtained satisfactory rate constants in studying two hydrogen abstraction reactions of CH_2O with H and O[^{3}P] [24,25]. It is expected that they are applicable to the present reactions.

2. Computational methods

The geometries and vibrational frequencies of the stationary points (i.e., reactants, products, and transition states) are calculated at the UQCISD/6-311G(d,p) level. The minimum energy paths (MEP) [26–28] is obtained by the intrinsic reaction coordinate (IRC) calculations with a gradient step size of 0.05 $(amu)^{1/2}$ bohr. The harmonic vibrational frequencies as well as the force-constant matrixes at the selected points along the IRC are calculated at the same level of theory. Because of the importance of the reaction paths for the hydrogen-abstraction dynamical properties, the energies of each point along the IRC are refined by the multicoefficient Gaussian 3-version 3s (MCG3/3) [29,30] method. GAUSSIAN 03 program [31] was applied to all of these electronic structure calculations.

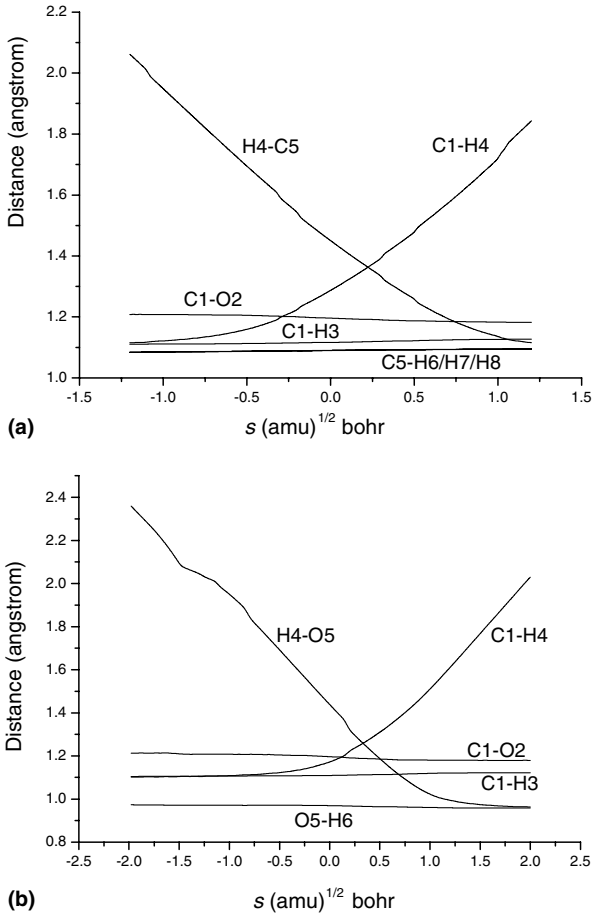

Fig. 2. (a) Changes of the interatomic distances (in nm) as functions of s $(amu)^{1/2}$ bohr at the UQCISD/6-311G(d,p) level for the $CH_2O + CH_3 \rightarrow CHO + CH_4$ reaction. (b) Same as those in (a) except for the $CH_2O + OH \rightarrow CHO + H_2O$ reaction.

Table 2
Total energies (E) of all the stationary points at the UQCISD/6-311(d,p) optimized geometries (in Hartree)

Species	UQCISD		MCG3/3
	E	E + ZPE	
OH	−75.5864933	−75.577857	−76.16311452
H_2O	−76.2716991	−76.249871	−76.86851281
CHO	−113.605001	−113.591901	−114.4764187
CH_2O	−114.249549	−114.222614	−115.1325471
CH_3	−39.7291633	−39.699435	−40.03969408
CH_4	−40.4016428	−40.356552	−40.72298906
$CH_2O\cdots OH$(HBC)	−189.8392	−189.80227	−191.2992149
TS1(CH_3)	−153.959495	−153.903815	−155.1571658
TS2(OH)	−189.831833	−189.797602	−191.2952951

Table 3
Forward and reverse reaction potential barrier (in kcal/mol)

	$CH_2O + CH_3 \rightarrow CHO + CH_4$			$CH_2O + OH \rightarrow CHO + H_2O$		
	ΔE^f	ΔE^r	$\Delta E^f - \Delta E^r$	ΔE^f	ΔE^r	$\Delta E^f - \Delta E^r$
UQCISD	12.06	29.59	−17.53	2.64	28.16	−25.52
UQCISD + ZPE	11.44	28.01	−16.57	1.80	27.72	−25.92
MCG3/3	9.46	26.51	−17.05	0.21	31.15	−30.94
Expt	7.90 [37]			0.175 ± 0.03 [11]		
UMP2/6-311G(d,p)	10.60 [17]		−16.00 [17]	1.20 [18]		
MCSCF				3.60 [19]		−21.70 [19]

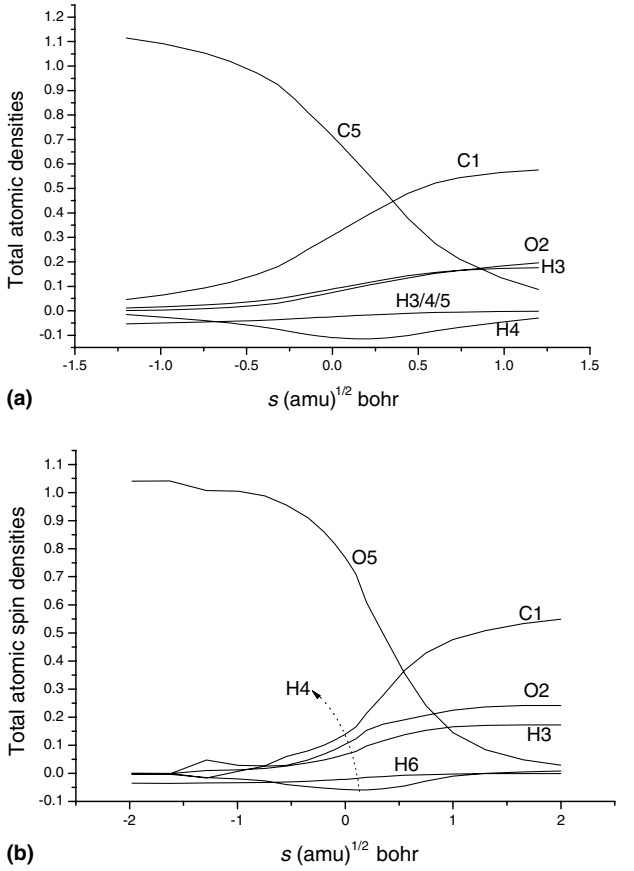

Fig. 3. (a) Changes of total atomic spin densities as functions of s $(amu)^{1/2}$ bohr at the UQCISD/6-311G(d,p) level for the $CH_2O + CH_3 \rightarrow CHO + CH_4$ reaction. (b) Same as those in (a) except for the $CH_2O + OH \rightarrow CHO + H_2O$ reaction.

The theoretical rate constants in the temperature range from 300 to 3000 K are calculated using the conventional transition state theory (TST), canonical variational transition state theory (CVT) and canonical variational transition state incorporating a small-curvature tunneling correction (CVT/SCT) method by POLYRATE 7.4 program [32]. In the calculation, the Euler single-step integrator with a step size of 0.0001 $(amu)^{1/2}$ bohr is used to follow the MEP, and the generalized normal-mode analysis was performed every 0.01 $(amu)^{1/2}$ bohr. The curvature components were calculated using a quadratic fitting to obtain the derivative of the gradient with respect to the reaction coordinate.

3. Results and discussion

3.1. Stationary points

The optimized parameters of the reactants (CH_2O and CH_3OH), the hydrogen-bonded complex (HBC) (at the reactant side) of reaction (2), transition states and products (CHO, H_2O and CH_4) at the UQCISD/6-311G(d,p) level are shown in Fig. 1 along with the available experimental data [33]. The largest deviation between the theoretical bond lengths (r) and the experimental values is 0.017 Å for r(C–H) in CH_4 and the largest deviation of the bond angles ($\angle$) is 0.2° for $\angle$OCH in CHO. Thus, it is obvious that the optimized bond lengths of the reactants and products are in good agreement with the experimental data [33]. The transition states TS1 and TS2, found in reactions (1) and (2), respectively, have the C_s symmetry. At the reactant side of reaction (2), the bond C1–O5 of the HBC is 3.243 Å, and it is so long that it can be rotated freely to any structure favorite to further connect with TS2. In the transition state structures, the distances of the bond C1–H4, which will be broken, increase by 16% and 6% with respect to the equilibrium bond distances of CH_2O in reactions (1) and (2), respectively. The C5–H4 distances, that will be formed, are 1.3 and 1.5 times as large as the equilibrium bond length of the methane and water molecule, respectively. Therefore, the two transition states are all reactant-like, and the hydrogen reactions will proceed via the early transition states.

The harmonic vibrational frequencies of the reactants, HBC, products and transition state at the UQCISD/6-311G(d,p) level are listed in Table 1. The frequencies have been scaled using a scale factor of 0.9537 [34] for the QCISD method. As seen in this table, most of the calculated frequencies are in good agreement with those of the available experimental values [35,36], and the maximum deviation is about 202 cm^{-1}. For the ground state CH_2O, the calculated C–H stretching, C–O stretching and $-CH_2$ bending frequencies are lower than the experimental values by 4.5%, 2.7%, 2.4%, respectively. For each transition state, the characteristic of the saddle point is confirmed by normal-mode analysis, which yields only one imaginary frequency whose eigenvector corresponds to the direction of the reaction.

Table 2 lists the total energies of the reactants, HBC, products and transition states at the UQCISD/6-311G(d,p), and MCG3/3 methods. Table 3 gives the reaction heats and the forward and reverse barriers of these two reactions at the different methods. For the purpose of comparison, the experimental values and the recent theoretical results are also listed in Table 3. The results show that, the hydrogen-bonded complex (HBC) at the reactant side of the reaction of CH_2O with OH with an energy value less than that of the reactants. It can be seen that the calculated reaction potential barriers by the MCG3/3 method are 9.46 and 0.21 kcal/mol for reactions (1) and (2), respectively, which are higher than the experimental values [37,11] and lower than the previous theoretical ones obtained by the UMP2/6-311G(d,p) [17,18] and MCSCF [19] methods. Since the forward barriers are far less than the reverse barriers, the forward reaction proceeds more easily than the reverse reaction for each reaction. In addition, the reac-

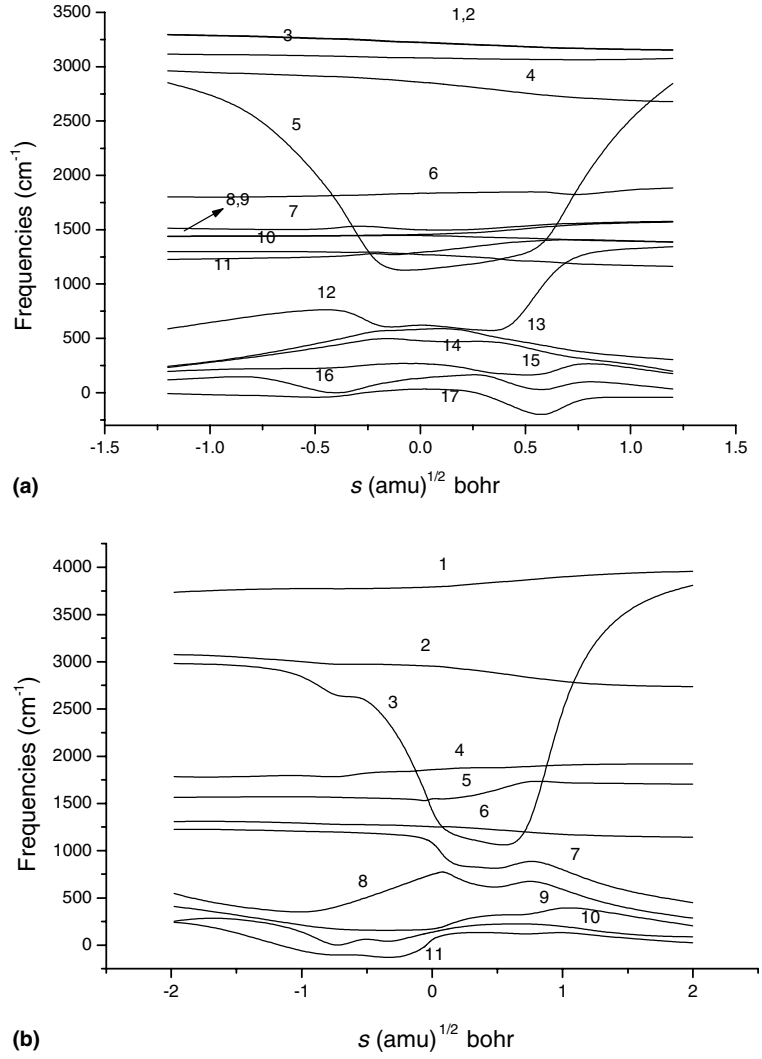

Fig. 4. (a) Changes of the generalized normal-mode vibrational frequencies at the UQCISD/6-311G(d,p) level for the $CH_2O + CH_3 \rightarrow CHO + CH_4$ reaction. (b) Same as those in a except for the $CH_2O + OH \rightarrow CHO + H_2O$ reaction.

tion heats of reactions (1) and (2) are −17.05 and −30.94 kcal/mol in the MCG3/3 method, respectively, so they are strong exothermic reactions.

3.2. Reaction path properties

Fig. 2 shows the bond length changes along the MEP of the reactions as functions of the reaction coordinate s $(amu)^{1/2}$ bohr at the UQCISD/6-311G(d,p) level for reactions (1) and (2), respectively. For reaction (1) in Fig. 2(a), it is obvious that the bond lengths, C1–H4 and C5–H4, change strongly in the course of reaction. The bond that broke, C1–H4, elongates after $s = -0.75$ $(amu)^{1/2}$ bohr. The C5–H4 bond rapidly shortens from reactants side and arrives at the equilibrium bond length of CH_4 at about $s = 1.0$ $(amu)^{1/2}$ bohr. It appears the geometric changes mainly take place in the region from about $s = -0.75$–1.0 $(amu)^{1/2}$ bohr. In addition, The C1–H3 and C1–O2 bond lengths during the course of reaction are almost same as the equilibrium bond lengths of CH_2O. For reaction (2) in Fig. 2(a), the geometric change is similar to that of reaction (1) and the key bond change takes place in the region from about $s = -0.5$–1.0 $(amu)^{1/2}$ bohr. Some one defined the "effective reaction region" as a region of the new bond forming and the old bond breaking. This region is delimited on the MEP where the geometrical structure of reaction molecules would change mightily. So it can be realized that the effective reaction regions for the two reactions about are −0.75–1.0 and −0.5–1.0 $(amu)^{1/2}$ bohr, respectively. It was found that the rupture of old bonds and formation of new bond for the two hydrogen abstraction reactions are both concerted.

The changes of total atomic spin densities of reaction (1) are given in Fig. 3(a). It can be seen that the total

atomic spin densities of C1 and C4 change greatly in the course of reaction, which means that, as the reaction proceeds, the unpaired electron moves from C5 to C1. However, the atomic spin densities of the O2, H3, H4, H6/7/8 atoms only have very small changes. It indicates that the H4 abstraction process has a little influence to the bond lengths C1–H3 and C1–O2 in the course of reaction. Fig. 3(b) shows the total atomic spin densities along the IRC for reaction (2). The O5 and C1 have the maximum spin densities in the reactant side and product side, respectively. It implies the unpaired electron moves from O5 to C1 in the course of reaction, which is similar to reaction (1).

The vibrational frequencies of generalized normal modes are shown in Fig. 4(a) and (b) as functions of the reaction coordinate*s* at the UQCISD/6-311G(d,p) level. In the negative limit of *s*, the frequencies are associated with the reactants $CH_2O + CH_3$, $CH_2O + OH$, respectively, and in the positive limit of *s*, the frequencies are associated with the products $CHO + CH_4$, $CHO + H_2O$, respectively. In the vicinity of the transition state, there are 17 and 11 real vibrational frequencies for reactions (1) and (2), respectively. In Fig. 4(a), the frequency curve of the modes (1)–(4), (6), (8)–(11) almost unchanged, because there is only small variation for the structure of CHO and CH_3 in the proceeding of the hydrogen abstraction reaction. The modes (7) and (11) are the degenerate bending vibrations with respect to C5–H6–H7–H8 and C1–H3–H4 on the reactants side, and they transform to degenerate bending vibrations with respect to C5–H4–H6–H7–H8 and C1–H2 on the products side, respectively. The frequency curve of mode (5) has the greatest variation in the course of reaction because it connects the frequency of the C1–H4 stretching vibration of CH_2O with the frequency of the C5–H4 stretching vibration of CH_4. Therefore, the mode (5) is the reactive mode in the hydrogen abstraction reaction, and its frequency has a significant change in the region $s = -0.75$–1.0 $(\text{amu})^{1/2}$ bohr as the reaction proceeds. Fig. 4(b) is similar to Fig. 4(a), we can see that the mode (3), which signifies the concerted process of the bond C1–H4 breaking and the bond O5–H4 forming, can be referred to as the reactive mode in the hydrogen abstraction reaction, and its reaction region is $s = -0.5$–1.0 $(\text{amu})^{1/2}$ bohr. So by discussing the changes of vibrational mode for the two reactions, it can be found that there exists a reactive vibrational mode, and its frequencies change is relevant to the formation and rupture of the covalent bond.

3.3. Rate constants

The rate constants of both reactions (1) and (2) are calculated by variational transition state theory with small-curvature tunneling correction (CVT/SCT) method in the temperature range from 300 to 3000 K at the

Table 4
Rate constants ($cm^3\ mol^{-1}\ s^{-1}$) for the reactions of CH_2O with CH_3 and OH in the temperature range 300–3000 K in the MCG3/3 method

T (K)	$CH_2O + CH_3 \rightarrow CHO + CH_4$				$CH_2O + OH \rightarrow CHO + H_2O$				
	TST	CVT	CVT/SCT	Expt. [8]	TST	CVT	CVT/SCT	Expt. [5]	Expt. [6]	Expt. [16]
300	1.20×10^{-19}	1.19×10^{-19}	1.12×10^{-18}	1.59×10^{-17}	9.51×10^{-13}	8.49×10^{-13}	1.28×10^{-12}	2.20×10^{-12}	1.01×10^{-11}	
400	5.92×10^{-18}	5.91×10^{-18}	1.71×10^{-17}	8.91×10^{-17}	2.49×10^{-12}	2.39×10^{-12}	3.12×10^{-12}	4.05×10^{-12}	1.18×10^{-11}	
600	3.97×10^{-16}	3.96×10^{-16}	6.20×10^{-16}	1.20×10^{-15}	8.56×10^{-12}	8.42×10^{-12}	1.00×10^{-11}	9.95×10^{-12}	1.57×10^{-11}	
800	4.22×10^{-15}	4.21×10^{-15}	5.40×10^{-15}	8.23×10^{-15}	1.99×10^{-11}	1.97×10^{-11}	2.24×10^{-11}	1.92×10^{-11}	2.01×10^{-11}	
1000	2.07×10^{-14}	2.06×10^{-14}	2.41×10^{-14}	3.80×10^{-14}	3.81×10^{-11}	3.69×10^{-11}	3.87×10^{-11}	3.23×10^{-11}	2.47×10^{-11}	
1200	6.69×10^{-14}	6.67×10^{-14}	7.43×10^{-14}	1.35×10^{-13}	6.48×10^{-11}	5.12×10^{-11}	5.35×10^{-11}	4.97×10^{-11}	2.95×10^{-11}	
1500	2.49×10^{-13}	2.48×10^{-13}	2.66×10^{-13}	6.51×10^{-13}	1.24×10^{-10}	7.98×10^{-11}	8.29×10^{-11}	8.44×10^{-11}	3.70×10^{-11}	1.08×10^{-10}
1600	3.56×10^{-13}	3.55×10^{-13}	3.77×10^{-13}	1.03×10^{-12}	1.49×10^{-10}	9.13×10^{-11}	9.47×10^{-11}	9.84×10^{-11}	3.96×10^{-11}	1.24×10^{-10}
1700	4.95×10^{-13}	4.93×10^{-13}	5.20×10^{-13}	1.58×10^{-12}	1.78×10^{-10}	1.04×10^{-10}	1.08×10^{-10}	1.14×10^{-10}		1.39×10^{-10}
2000	1.15×10^{-12}	1.15×10^{-12}	1.19×10^{-12}	5.05×10^{-12}	2.83×10^{-10}	1.48×10^{-10}	1.53×10^{-10}	1.68×10^{-10}		1.84×10^{-10}
2200	1.85×10^{-12}	1.84×10^{-12}	1.90×10^{-12}		3.72×10^{-10}	1.84×10^{-10}	1.89×10^{-10}	2.11×10^{-10}		2.12×10^{-10}
2500	3.40×10^{-12}	3.39×10^{-12}	3.47×10^{-12}		5.34×10^{-10}	2.47×10^{-10}	2.53×10^{-10}	2.87×10^{-10}		
3000	7.80×10^{-12}	7.77×10^{-12}	7.89×10^{-12}		8.91×10^{-10}	3.78×10^{-10}	3.87×10^{-10}			

MCG3/3 method. For comparison in the same temperature, Table 4 also lists the computational rate constants at the TST, CVT, and CVT/SCT theories over a broad temperature from 300 to 3000 K, together with the recent measured experimental results [5,6,8,16]. For the each reactions, the difference between the values of TST rate constants and those of CVT rate constants in the whole temperature range is small, which enables us to conclude that the variational effect is very small or almost negligible. However, the CVT/SCT rate constants are significantly larger than the CVT rate constants in the lower temperature range and they are asymptotic to the CVT ones at the higher temperatures, which means only in the lower temperature ranges does the small-curvature tunneling (SCT) correction effect play an important role for the reactions. For example, for reaction (1), the CVT/SCT rate constants at 300 K are 9.3 times the TST and the CVT rate constants. At 800 and 3000 K, the multiplying factors are 1.28 and 1.01, respectively.

In addition, in comparison with the rate constants of TST and CVT in the experimentally measured temperature ranges, the CVT/SCT rate constants are in much better agreement with the corresponding experimental values for reactions. The same results can be seen clearly from Fig. 5(a) and (b), in which the theoretical and available experimental rate constants for the reactions are plotted against $1000/T$ within 300–3000 K. For reaction (1), from Table 4 and Fig. 5(a), one can see that the CVT/SCT rate constants agree well with the

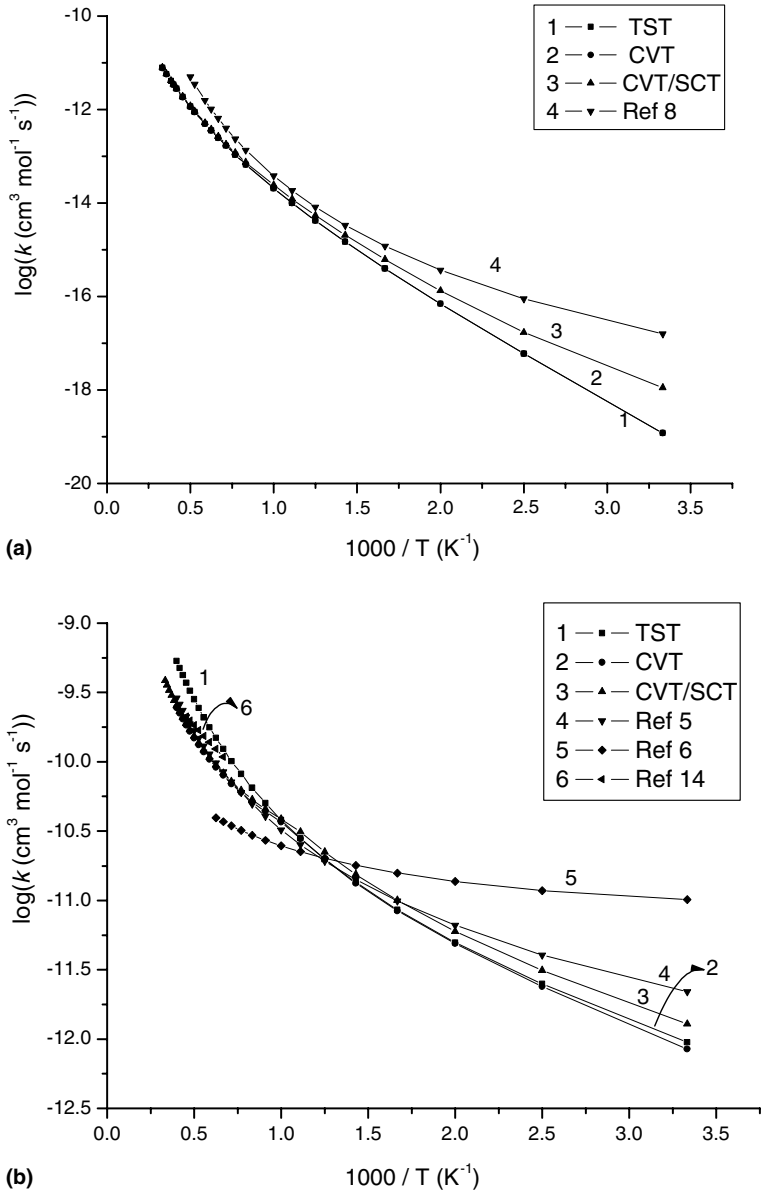

Fig. 5. (a) Plot of the calculated rate constants k ($cm^3\ mol^{-1}\ s^{-1}$) in the MCG3/3 method and available experimental data versus $1000/T$ in 300–3000 K for the $CH_2O + CH_3 \rightarrow CHO + CH_4$ reaction. (b) Same as those in (a) except for the $CH_2O + OH \rightarrow CHO + H_2O$ reaction.

experimental values obtained by Tarun et al. [8] in the temperature range from 400 to 2000 K, but a moderate deviation from the experimental values from 300 to 400. For the reaction (2), the rate constants calculated by CVT/SCT method are in good agreement with experimental data from [5,16] within the range of measured temperatures. In comparison with experimental data from [6], they deviate about a factor from at the low temperature range but are agreement approximately at the high temperature. Based on the calculated rate constants in Table 4, the data is fitted using a standard nonlinear least-squares fitting procedure in the temperature range of 300–3000 K. The expressions of the rate constants are $k_1 = 4.09 \times 10^{-25} T^{3.92} \exp(-2324.7/T)$ $\mathrm{cm^3\,mol^{-1}\,s^{-1}}$ and $k_2 = 1.55 \times 10^{-16} T^{1.85} \exp(-463.0/T)$ $\mathrm{cm^3\,mol^{-1}\,s^{-1}}$ for the reactions $CH_2O + CH_3 \rightarrow CHO + CH_4$ and $CH_2O + OH \rightarrow CHO + H_2O$, respectively.

4. Conclusion

The hydrogen abstraction reactions of CH_2O with CH_3 and OH have been investigated theoretically by an ab initio direct dynamics method. The UQCISD/6-311G(d,p) method can provide accurate geometry and reasonable frequency information. By the MCG3/3 method, the forward barrier heights with zero-point energy are obtained to be 9.46 and 0.21 kcal/mol for reactions (1) and (2), respectively. The changes of the geometry and reactive normal mode vibrational frequencies along the IRC mainly take place in the region $s = -0.75$–1.0 and -0.5–1.0 $(\mathrm{amu})^{1/2}$ bohr for reactions (1) and (2), respectively. The CVT/SCT rate constants are in good agreement with the experimental values over all the measured temperature range. The variational effect is weak, and the small curvature tunneling correction makes an important contribution to the calculation of rate constants in the lower temperature range for the reactions. The rate constants at the 300–3000 K are fitted by the three parameter expression: $k_1 = 4.09 \times 10^{-25} T^{3.92} \exp(-2324.7/T)$ $\mathrm{cm^3\,mol^{-1}\,s^{-1}}$ and $k_2 = 1.55 \times 10^{-16} T^{1.85} \exp(-463.0/T)$ $\mathrm{cm^3\,mol^{-1}\,s^{-1}}$ for the reactions CH_2O with CH_3 and OH, respectively. To conclude, the reaction mechanism of hydrogen abstraction reactions of CH_2O with CH_3 and OH are better described by reaction paths and rate constants using QCISD/6-311(d,p) and CVT/SCT theoretical methods.

Acknowledgement

The work is supported by the National Nature Science Foundation of China and the Young Teacher Foundation of Beijing University of Chemical Technology (QN0308).

References

[1] K.T. Choudhury, M.C. Lin, Combust. Sci. Tech. 64 (1989) 19.
[2] C.K. Westbrook, F.L. Dryer, Combust. Sci. Tech. 20 (1979) 125.
[3] T.S. Norton, F.L. Dryer, Combust. Sci. Tech. 63 (1989) 107.
[4] T.B. Hunter, H. Wang, T.A. Litzinger, M. Frenklach, Combust. Flame 97 (1994) 201.
[5] S. Zabarnick, J.W. Fleming, M.C. Lin, Int. J. Chem. Kinet. 20 (1988) 117.
[6] W. Tsang, R.F. Hampson, J. Phys. Chem. Ref. Data. 15 (1986) 1087.
[7] S. Hochgerb, F.L. Dryer, Combust. Flame 91 (1992) 257.
[8] K.T. Choudhury, W.A. Sanders, M.C. Lin, J. Phys. Chem. 93 (1989) 5143.
[9] K.C. Manthorne, P.D. Pacey, Can. J. Chem. 56 (1978) 1307.
[10] A.M. Held, K.C. Manthorne, P.D. Pacey, H.P. Remholdt, Can. J. Chem. 55 (1977) 471.
[11] R. Atkinson, J.N. Pitts, J. Chem. Phys. 68 (1978) 3581.
[12] L.J. Stief, D.F. Nava, W.A. Payen, J.V. Michael, J. Chem. Phys. 73 (1980) 2254.
[13] F. Temps, H.Gg. Wagner, Ber. Bunsen-Ges. Phys. Chem. 88 (1984) 415.
[14] E.D. Morris Jr., H. Niki, J. Chem. Phys. 55 (1971) 1991.
[15] J. Peeters, G. Mahnen, Symp. Proc. Combust. Pittsburgh 14 (1973) 133.
[16] C.T. Bowman, Combust. Flame 25 (1975) 343.
[17] Y. Su, J.S. Francisco, Chem. Phys. Lett. 236 (1995) 162.
[18] J.S. Francisco, J. Chem. Phys. 96 (1992) 7597.
[19] R.S. Maribel, M. Page, J. Phys. Chem. 94 (1990) 3242.
[20] D.G. Truhlar, B.C. Garrett, Acc. Chem. Res. 13 (1980) 440.
[21] D.G. Truhlar, A.D. Isaacson, B.C. Garrett, in: M. Baer (Ed.), Theory of Chemical Reaction Dynamics, CRC Press, Boca Raton, FL, 1985, p. 65.
[22] D.G. Truhlar, B.C. Garrett, Ann. Rev. Phys. Chem. 35 (1984) 159.
[23] Y.-P. Liu, G.C. Lynch, T.N. Truong, D.-H. Lu, D.G. Truhlar, B.C. Garrett, J. Am. Chem. Soc. 115 (1993) 2415.
[24] H.Y. Li, W.L. Feng, Y.Q. Ji, Z.F. Xu, Acta Chim. Sinica 59 (2001) 1413.
[25] H.Y. Li, W.L. Feng, Y.Q. Ji, Z.F. Xu, M. Lei, Acta Phys. -Chim. Sinica 18 (2002) 446.
[26] K. Fukui, J. Phys. Chem. 74 (1970) 4161.
[27] C. Gonzalez, H.B. Schlegel, J. Chem. Phys. 90 (1989) 2154.
[28] C. Gonzalez, H.B. Schlegel, J. Phys. Chem. 94 (1990) 5523.
[29] B.J. Lynch, D.G. Truhlar, J. Phys. Chem. 107 (2003) 3898.
[30] B.J. Lynch, Y. Zhao, D.G. Truhlar, J. Phys. Chem. 107 (2003) 1384.
[31] M.J. Frisch, G.W. Trucks, H.B. Schlegel, G.E. Scuseria, M.A. Robb, J.R. Cheeseman, J.A. Montgomery, Jr., T. Vreven, K N. Kudin, J.C. Burant, J.M. Millam, S.S. Iyengar, J. Tomasi, V. Barone, B. Mennucci, M. Cossi, G. Scalmani, N. Rega, G.A. Petersson, H. Nakatsuji, M. Hada, M. Ehara, K. Toyota, R. Fukuda, J. Hasegawa, M. Ishida, T. Nakajima, Y. Honda, O. Kitao, H. Nakai, M. Klene, X. Li, J.E. Knox, H.P. Hratchian, J.B. Cross, C. Adamo, J. Jaramillo, R. Gomperts, R.E. Stratmann, O. Yazyev, A.J. Austin, R. Cammi, C. Pomelli, J.W. Ochterski, P.Y. Ayala, K. Morokuma, G.A. Voth, P. Salvador, J.J. Dannenberg, V.G. Zakrzewski, S. Dapprich, A.D. Daniels, M.C. Strain, O. Farkas, D.K. Malick, A.D. Rabuck, K. Raghavachari, J.B. Foresman, J.V. Ortiz, Q. Cui, A.G. Baboul, S. Clifford, J. Cioslowski, B.B. Stefanov, G. Liu, A. Liashenko, P. Piskorz, I. Komaromi, R.L. Martin,; D.J. Fox, T. Keith, M.A. Al-Laham, C.Y. Peng, A. Nanayakkara, M. Challacombe, P.M. W. Gill, B. Johnson, W. Chen, M.W. Wong, C. Gonzalez, J.A. Pople, Gaussian 03, Revision B.04, Gaussian, Inc., Pittsburgh, PA, 2003.
[32] R. Steckler, X.Y. Chuang, D.G. Truhlar, et al. POLYRATE version 7.4, University of Minnesota, MN, 1997.

[33] K. Yamada, T. Nakagawa, K. Kuchitsu, Y. Morine, J. Mol. Spectrosc. 38 (1971) 70.
[34] A.P. Scott, L. Radom, J. Phys. Chem. 100 (1996) 16502.
[35] K.K. Murray, T.M. Miller, D.G. Leopold, W.C. Lineberger, J. Chem. Phys. 84 (1986) 2520.
[36] D.E. Reisner, R.W. Field, J.L. Kinsey, H.L. Dai, J. Chem. Phys. 80 (1984) 5968.
[37] J.A. Kerr, M.J. Parsonage, Evaluated Kinetic Data on Gas Phase Hydrogen Transfer Reactions of MetButterworth, Butterworth, London, 1976.